J Mater Sci: Mater Electron (2018) 29:1232–1237
DOI 10.1007/s10854-017-8025-9

Easy hydrothermal synthesis of multi-shelled La_2O_3 hollow spheres for lithium-ion batteries

Shaohua Qu[1] · Yinkai Yu[1] · Kejun Lin[1] · Peiyu Liu[1] · Chenhui Zheng[1] · Liuding Wang[1] · Tingting Xu[2] · Zhengdong Wang[3] · Hongjing Wu[1]

Received: 15 September 2017 / Accepted: 9 October 2017 / Published online: 20 October 2017

Abstract Herein, uniform triple-shelled La_2O_3 hollow spheres were synthesized for the first time by a facile one-pot hydrothermal method capable of controlling the number of internal thin-shells, which can be achieved by controlling the calcination temperature. Used as anodes for Li-ion batteries, the triple-shelled La_2O_3 hollow spheres show excellent cycling performance, good rate capacity, and high specific capacity. A superior capacity, up to 108 mAh g^{-1} with minimal irreversible capacity after 100 cycles is achieved at a current rate of 100 mA g^{-1}. After the high-rate charge–discharge cycling, a specific discharge capacity as high as 190.1 mAh g^{-1} can be restored when the current density is reduced to 50 mA g^{-1} (theoretical specific capacity = 246.8 mAh g^{-1}).

1 Introduction

With the more and more growing development of lithium-ion batteries (LIBs), the great demand for high capacity and stability of LIBs has become more and more attractive. A large number of researchers have paid attention to these anode materials for decades to improve the specific capacity of LIBs, attempting a variety of metal oxides. They have made major progress. For example, when TiO_2 [1], Fe_2O_3 [2], Co_3O_4 [3], Mn_2O_3 [4], CuO [5] and NiO [6] have been introduced as anode materials, they show high capacities. At the same time, they also suffer from some restrictions, such as poor stability, the high mass density and short lifetime. Recently, various micro-/nanostructures of metal oxides have been introduced for breaking through the barriers. On account of the high specific surface area and special structure, they reveal preferable cycling performance.

La is considered as one of the most important element in the rare earths. And due to the high chemical stability and low toxicity, it gets preferable applications in the field of civil and military, such as rare earth glass, ceramics, catalyst, fluorescent powder, laser, cathode materials and so on [7, 8]. Compared with other elements in rare earths, the storage of La_2O_3 is higher while the usage is lower, that is unbalanced in the extreme. And we find that there are poor document literatures about La_2O_3 when it is used as the anode materials of LIBs, so it is necessary for us to search for a new application pattern of La_2O_3 urgently. Sacrificial template method was used to fabricate the La_2O_3 hollow nanospheres [9]. However, to the best of our knowledge, controlled synthesis of multi-shelled La_2O_3 hollow spheres is still a challenging task due to their unique properties. What's more, lanthanum ion (La^{3+}) substituted $CoFe_2O_4$ anode material for lithium ion battery applications shows the higher charge/discharge performances of half cells [10].

Based on the above statements, we report a novel, one-pot approach for the preparation of multi-shelled La_2O_3 hollow spheres by chemically induced self-assembly in the hydrothermal environment. The obtained La_2O_3 hollow spheres were used as the anode materials of LIBs, and they reveal the novel cycling performance, such as quickly charge/discharge

---

✉ Tingting Xu
Tingtingxu@nwpu.edu.cn

✉ Hongjing Wu
wuhongjing@mail.nwpu.edu.cn

[1] Department of Applied Physics, Northwestern Polytechnical University, Xi'an, People's Republic of China

[2] Department of Applied Chemistry, Northwestern Polytechnical University, Xi'an, People's Republic of China

[3] Center of Nanomaterials for Renewable Energy (CNRE), State Key Laboratory of Electrical Insulation and Power Equipment, School of Electrical Engineering, Xi'an Jiaotong University, Xi'an, People's Republic of China

rate and stable cycling performance. Based on these advantages, we are expected to make it more practical application. More importantly, this novel facile method may become a general synthetic approach for fabricating multi-shelled hollow nanostructures of other rare-earth elements materials and it can provide a new usage for all the rare-earth elements materials.

2 Experimental

2.1 Synthesis

D-glucose monohydrate purchased from the National Reagent Corp. (Shanghai, China) was used as a carbon source. Lanthanum nitrate hexahydrate ($La(NO_3)_3 \cdot 6H_2O$) was obtained from Aladdin Industrial Corporation (Shanghai, China).

The multi-shelled La_2O_3 hollow spheres were prepared by the following one-pot process [11–14]. Firstly, precursor solution was obtained by dissolving the required amount of the D-glucose and lanthanum nitrate for 0.5 h-vigorous stirring (G:M = 1:1.85). Then the solution was transferred to a 100 ml capacity Teflon-lined stainless-steel autoclave at 180 °C for 20 h. Followed filtered and repeatedly washed with distilled water and ethanol, the derived precipitate were dried at 80 °C for 12 h. In order to remove the carbonaceous template as well as to crystallize the multi-shelled La_2O_3 hollow spheres, the composite particles were heated to 550 °C for 3 h in a muffle furnace in air. Furthermore, for researching the influence of the temperature and the formation process of the multi-shelled La_2O_3 hollow spheres, the samples calcined at 270, 350, 430, 500 °C and the uncalcined sample were prepared, respectively.

2.2 Characterization

The microscopic size and morphology of the obtained products were analyzed by using a FEI Quanta 600 FEG scanning electronic microscope (SEM) and a FEI Tecnai G^2 F30 transmission electron microscope (TEM). Crystallographic phases of the products were investigated by powder X-ray diffraction (XRD) (Rigaku D/Max 2500).

2.3 Electrochemical measurements

La_2O_3, acetylene black and polyvinylidene fluoride binder in *N*-methylpyrrolidone with a weight ratio of 70:20:10 was taken as the working electrode slurry for casting. The slurry was cast on the Cu foil followed by drying at 80 °C in a vacuum oven for 12 h prior to coin cell (CR 2023) assembly in an argon-filled glove box. Lithium foil was used as a counter electrode and a polypropylene film as the separator. The electrolyte was made from 1 M $LiPF_6$ in ethylene carbonate and diethyl carbonate (1:1 by volume). The charging/discharging behavior of all the cells was galvanostatically cycled between 3.00 and 0.01 V. Capacity retention tests of the assembled cells were carried out for the required rates. Rate capability tests of the cells were performed by changing the rate from 50 to 2000 mA g^{-1} for each five cycles.

3 Results and discussion

3.1 Phase and morphology of the samples

The formation of La_2O_3 nanoparticles were analyzed by using wide-angle X-ray diffractometer (see Fig. 1). The observed diffraction pattern of La_2O_3 was matched well with the hexagonal La_2O_3 crystalline phase which was confirmed by comparing the observed diffraction pattern with standard JCPDS data (JCPDS #40-1279). There are three strong peaks around $2\theta = 29.3°$, 38.1°, and 44.3°, assigned to (10−1), (10−2), and (110) reflections of La_2O_3 (*P-3m1*(164), $a = 4.039$, $c = 6.403$). However, other peaks near $2\theta = 22°$, 31°, and 41° may be attributed to the cubic La_2O_3 phase (JCPDS #65-3185), which leads to the mismatch between the measured XRD pattern and the standard JCPDS data.

The morphology of the La_2O_3 calcined at different temperatures is shown in Fig. 2, displaying a highly uniform distribution. As shown in the Fig. 2a, b, the solid spheres are obtained when the La_2O_3 precursors are calcined at 270 and 350 °C, respectively. The surface of these solid spheres with the diameter of approximate 1–2 µm is fairly smooth, indicating these solid spheres possess compact structure. What's more, we find that the diameter of these solid spheres will shrink with increasing the calcination temperature, and we can catch sight of it obviously at the high calcination

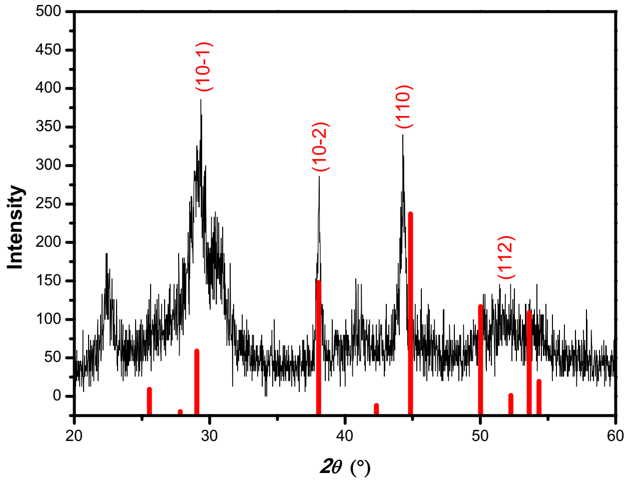

Fig. 1 XRD pattern of the La_2O_3 calcined at 430 °C

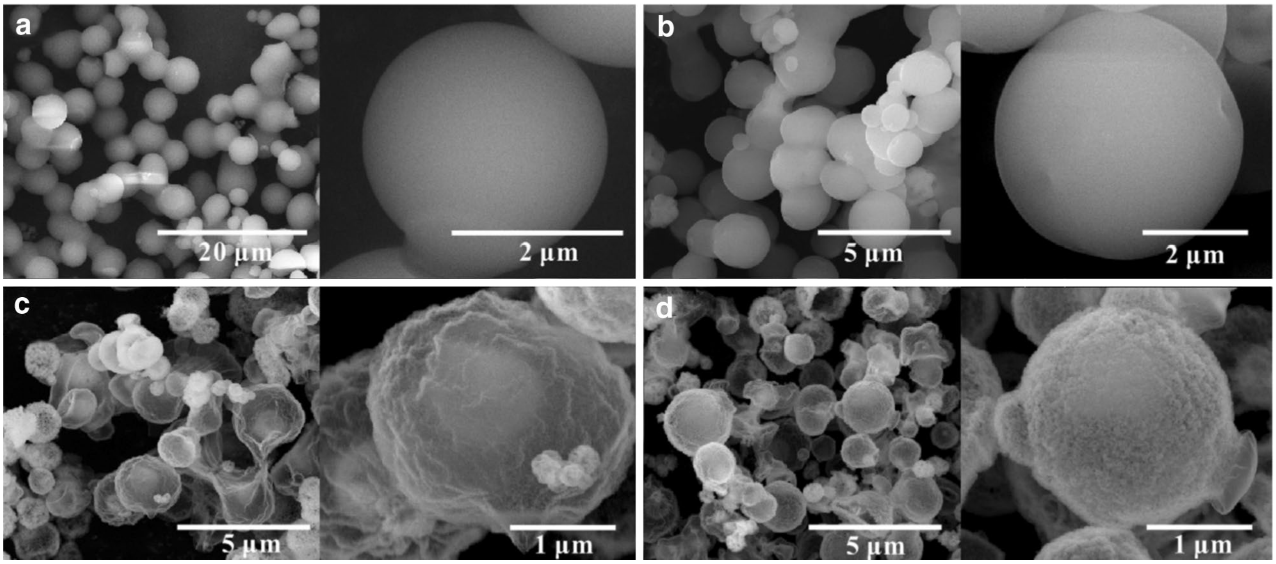

Fig. 2 FESEM images of multi-shelled La_2O_3 hollow spheres calcined at different temperatures: **a** 270 °C, **b** 350 °C, **c** 430 °C, and **d** 550 °C (enlarged right)

temperature. This phenomenon is also observed in the previous paper [15] and it is attributed to its reaction mechanism. When the calcination temperature is higher than 300 °C, the carbon contained in the solid spheres can be oxidized to carbon dioxide (CO_2) and carbon monoxide (CO) accompanied with the residual substance shrinking gradually [15].

Figure 2c exhibits multi-shelled La_2O_3 hollow spheres when the La_2O_3 precursors calcined at 430 °C. A thin La_2O_3 shell whose thickness is about several tens of nanometers set out to forming and a smaller solid sphere come into being as the core. From this, we infer that the core contained carbon can be considered as a template with its shrinking.

Interestingly, a special growth type is found in the process of forming. Consistent with its morphology, it's similar to the cell mitosis in the field of biology, but not dividing two spheres from a bigger sphere. Different from the formation of cobalt oxide (Co_3O_4) [16], tin oxide (SnO_2) [17], nickel oxide (NiO) [18] and other previous oxide [19–23], this phenomenon is the first time to be observed. It is ascribed to the special property and loosened structure.

When the temperature reaches up to 550 °C, its microscopic morphology is shown in Fig. 2d. Uniform spheres like as the head of garlic can be observed. In addition, these spheres are the typical structure of core–shell. The shell wrinkles severely, providing a higher specific surface area. Increasing the calcination temperature, these micro-spheres turn to fragment.

Figure 3 shows the TEM images of the La_2O_3 crystalline phase calcined at high temperatures. From their TEM images, the further structure can be comprehended. Figure 3a demonstrates that double-shelled La_2O_3 hollow spheres can be synthesized at 430 °C. From the amplified image (inset in Fig. 3a), the outer-shell made up of nanoparticles are shown in detail. These nanoparticles with a diameter of approximate 20 nm arrange loosely. It is attributed to reaction mechanism that La_2O_3 can release the CO_2 gas in the process of the reaction. At the same time, the formation process that is similar to the cell mitosis is shown in Fig. 3b. Figure 3c, d sheds light on the morphology when

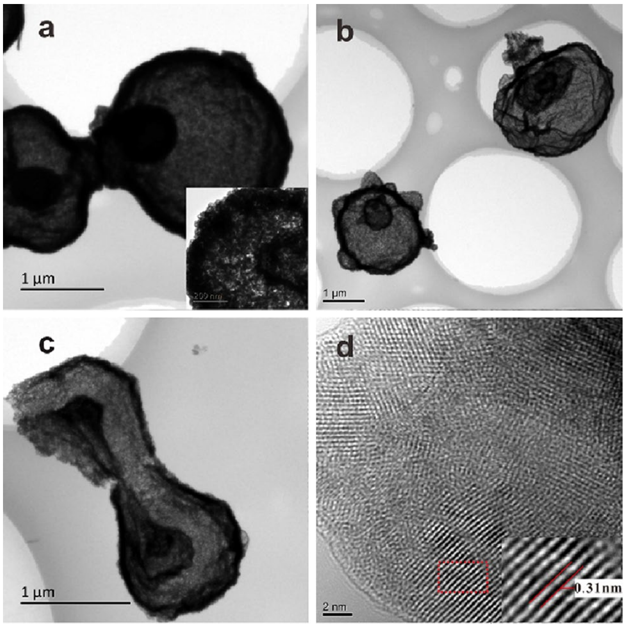

Fig. 3 TEM images of multi-shelled La_2O_3 hollow spheres calcined at different temperatures: **a** 430 °C, **b** 500 °C, and **c, d** 550 °C

the calcination temperature increases to 550 °C. The triple-shelled La_2O_3 hollow spheres start to contract sharply and a lot of fragment appears. It is consistent with the SEM images. In the crystallography, the strongest La_2O_3 (10−1) planes are observed, which is very consistent with the XRD results (Fig. 1). Compared with the widely used two-pot methods for creating metal oxide hollow spheres [3], the present one-pot hydrothermal approach provides a more facile route for large-scale synthesis of uniform multi-shelled La_2O_3 hollow spheres.

3.2 Electrochemical properties

Standard La_2O_3/Li half-cells were used to measure the lithium storage properties of the multi-shelled La_2O_3 hollow spheres as anodes. Figure 4 shows the cycling performance of the multi-shelled La_2O_3 hollow spheres at a current rate of 100 mA g^{-1} between 0.01 and 3.00 V for 100 cycles. After 100 cycles, the La_2O_3 hollow spheres calcined at 550 °C (triple-shelled La_2O_3 hollow sphere) show a higher capacity than the La_2O_3 hollow spheres calcined at lower temperatures. As shown, the specific discharge capacity of the triple-shelled La_2O_3 hollow spheres is around 121.6 mAh g^{-1} in the second cycle, and it is very stable with almost 100% capacity retention for at least 100 cycles. This cycling performance is remarkable compared to previously reported results for metal oxide electrodes [15, 24, 25]. The specific capacities of La_2O_3 materials calcined at 270 and 350 °C increased initially with cycling probably due to the gradual activation of the inner-side surface characteristics of the La_2O_3 hollow spheres [26]. After a certain number of cycles, the electrolyte slowly diffuses through the pores of the hollow spheres and subsequently interacts with the inner active components of the hollow spheres. This mechanism could account for the increase in the specific capacity of the La_2O_3 electrode.

Furthermore, the rate capacity is evaluated with current densities ranging from 50 to 2000 mAh g^{-1} (Fig. 5). As can be seen, the average specific capacities are 194.6, 163.8, 134.0, 99.6, 76.7, 54.5 mAh g^{-1} at the current densities of 50, 100, 200, 500, 1000, 2000 mA g^{-1}, respectively. After the high-rate charge–discharge cycling, a specific discharge capacity as high as 190.1 mAh g^{-1} can be restored when the current density is reduced to 50 mA g^{-1}. The above results clearly imply the potential lithium storage properties of triple-shelled La_2O_3 hollow spheres as an anode material for LIBs.

The impressive cycling stability and excellent rate performance of multi-shelled La_2O_3 hollow spheres could be attributed to the following aspects. First, the presence of small primary La_2O_3 nanoparticles and micropores can improve Li-ion transport, resulting in high capacity (theoretical specific capacity = 246.8 mAh g^{-1}) and excellent rate capability. Second, the unique triple-shell interior structure could buffer the large volume change associated with the repeated Li^+ insertion/extraction processes during cycling and keep the structural integrity, thus improving the cycling stability [27–29].

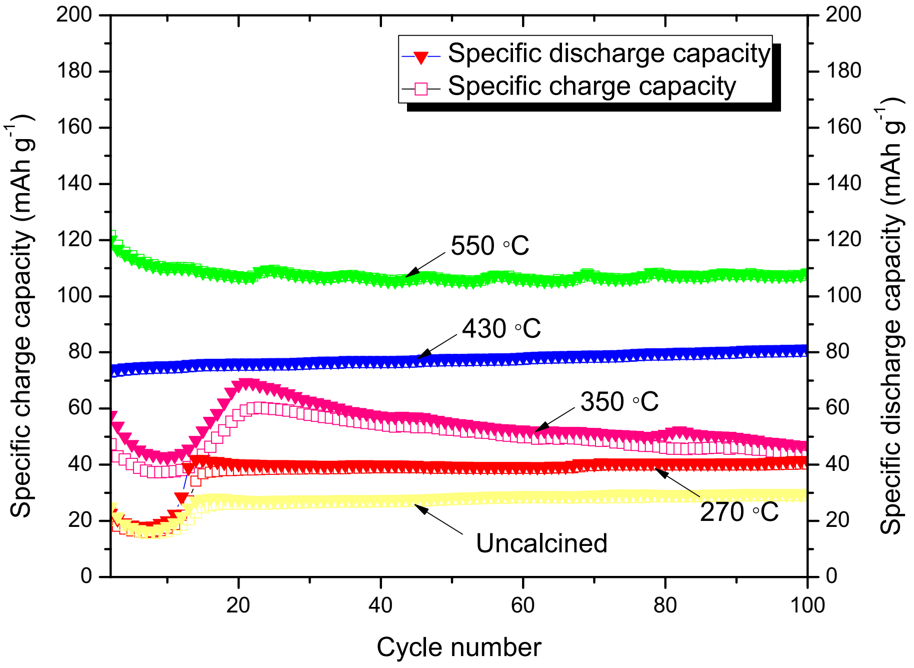

Fig. 4 Specific capacity versus cycle number curves for the battery fabricated with La_2O_3 anode materials

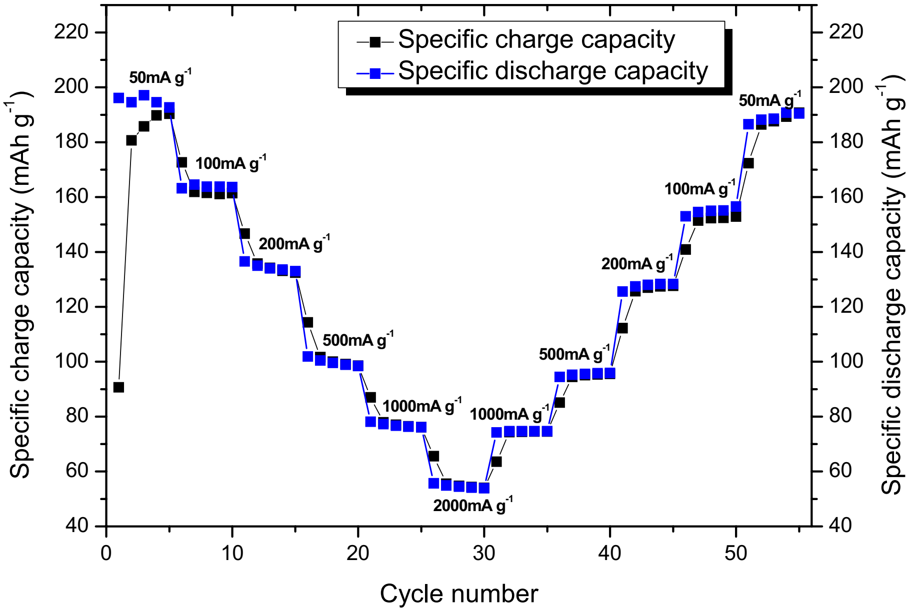

Fig. 5 Rate performance at various current densities of the triple-shelled La_2O_3 hollow sphere electrodes from 50 to 2000 mA g^{-1}

4 Conclusions

In summary, a facile one-pot hydrothermal method has been developed for the controllable synthesis of uniform multi-shelled La_2O_3 hollow spheres. The interior structure and size of the uniform multi-shelled La_2O_3 hollow spheres can be controlled by varying the calcination temperature. The resultant triple-shelled La_2O_3 hollow spheres exhibit a high initial reversible capacity of 121.6 mAh g^{-1} at a current density of 100 mA g^{-1}, and good cycling performance over 100 cycles. After the high-rate charge–discharge cycling, a specific discharge capacity as high as 190.1 mAh g^{-1} can be restored when the current density is reduced to 50 mA g^{-1} (theoretical specific capacity = 246.8 mAh g^{-1}).

Acknowledgements Financial support was provided by National Natural Science Foundation of China (Nos. 50771082 and 60776822). The project was also supported by Natural Science Basic Research Plan in Shaanxi Province of China (Program No. 2017JQ5116). The authors thank the colleagues in the laboratory of International Center for Dielectric Research for their support.

References

1. H. Ren, J. Sun, R. Yu, M. Yang, L. Gu, P. Liu, H. Zhao, D. Kisailuse, D. Wang, Controllable synthesis of mesostructures from TiO_2 hollow to porous nanospheres with superior rate performance for lithium ion batteries. Chem. Sci. **7**, 793–798 (2016)
2. Z. Wu, Y. Zhong, J. Li, X. Guo, L. Huang, B. Zhong, S. Sun, L-histidine-assisted template-free hydrothermal synthesis of α-Fe_2O_3 porous multi-shelled hollow spheres with enhanced lithium storage properties. J. Mater. Chem. A **2**, 12361–12367 (2014)
3. J. Wang, N. Yang, H. Tang, Z. Dong, Q. Jin, M. Yang, D. Kisailus, H. Zhao, Z. Tang, D. Wang, Accurate control of multishelled Co_3O_4 hollow microspheres as high performance anode materials in lithium-ion batteries. Angew. Chem. Int. Ed. **52**, 6417–6420 (2013)
4. H. Su, Y. Xu, S. Feng, Z. Wu, X. Sun, C. Shen, J. Wang, J. Li, L. Huang, S. Sun, Hierarchical Mn_2O_3 hollow microspheres as anode material of lithium ion battery and its conversion reaction mechanism investigated by XANES. ACS Appl. Mater. Interfaces **7**, 8488–8494 (2015)
5. J.C. Park, J. Kim, H. Kwon, H. Song, Gram-scale synthesis of Cu_2O nanocubes and subsequent oxidation to CuO hollow nanostructures for lithium-ion battery anode materials. Adv. Mater. **21**, 803–807 (2009)
6. P. Poizot, S. Laruelle, S. Grugeon, L. Dupont, J.M. Tarascon, Nano-sized transition-metal oxides as negative-electrode materials for lithium-ion batteries. Nature **407**, 496–499 (2000)
7. C.G. Hu, H. Liu, W.T. Dong, Y.Y. Zhang, G. Bao, C.S. Lao, Z.L. Wang, $La(OH)_3$ and La_2O_3 nanobelts—synthesis and physical properties. Adv. Mater. **19**, 470–474 (2007)
8. S. Shi, K. Li, S. Wang, R. Zong, G. Zhang, Structural characterization and enhanced luminescence of Eu-doped $2CeO_2$-$0.5La_2O_3$ composite phosphor powders by a facile solution combustion synthesis. J. Mater. Chem. C **5**, 4302–4309 (2017)
9. M. Sasidharan, N. Gunawardhana, M. Inoue, S. Yusa, M. Yoshiob, K. Nakashimac, La_2O_3 hollow nanospheres for high performance lithium-ion rechargeable batteries. Chem. Commun. **48**, 3200–3202 (2012)
10. R. Indhrajothi, I. Prakash, M. Venkateswarlu, N. Satyanarayan, Lanthanum ion (La^{3+}) substituted $CoFe_2O_4$ anode material for lithium ion battery applications. New J. Chem. **39**, 4601–4610 (2015)
11. G. Wu, Y. Cheng, F. Xiang, Z. Jia, Q. Xie, G. Wu, H. Wu, Morphology-controlled synthesis, characterization and microwave absorption properties of nanostructured 3D CeO_2. Mater. Sci. Semiconduct. Process. **41**, 6–11 (2016)
12. H. Wu, G. Wu, L. Wang, Peculiar porous α-Fe_2O_3, γ-Fe_2O_3 and Fe_3O_4 nanospheres: facile synthesis and electromagnetic properties. Powder Technol. **269**, 443–451 (2015)
13. G. Wu, Y. Cheng, Z. Wang, K. Wang, A. Feng, In situ polymerization of modified graphene/polyimide composite with improved

mechanical and thermal properties. J. Mater. Sci.: Mater. Electron. **28**, 576–581 (2017)

14. G. Wu, Y. Cheng, Y. Ren, Y. Wang, Z. Wang, H. Wu, Synthesis and characterization of γ-Fe_2O_3@C nanorod-carbon sphere composite and its application as microwave absorbing material. J. Alloys Compd. **652**, 346–350 (2015)
15. H. Wu, Y. Wang, C. Zheng, J. Zhu, G. Wu, X. Li, Multi-shelled NiO hollow spheres: easy hydrothermal synthesis and lithium storage performances. J. Alloys Compd. **685**, 8–14 (2016)
16. Y. Wang, A. Pan, Q. Zhu, Z. Nie, Y. Zhang, Y. Tang, S. Liang, G. Cao, Facile synthesis of nanorod-assembled multi-shelled Co_3O_4 hollow microspheres for high-performance supercapacitors. J. Power Sources **272**, 107–112 (2014)
17. Y. Lin, J. Duh, M. Hung, Shell-by-shell synthesis and applications of carbon-coated SnO_2 hollow nanospheres in lithium-ion battery. J. Phys. Chem. C **114**, 13136–13141 (2010)
18. H. Wu, G. Wu, Q. Wu, L. Wang, Facile synthesis and microwave absorbability of C@Ni-NiO core-shell hybrid solid sphere and multi-shelled NiO hollow sphere. Mater. Charact. **97**, 18–26 (2014)
19. H.L. Lv, X.H. Liang, G.B. Ji, H.Q. Zhang, Y.W. Du, Porous three-dimensional flower-like Co/CoO and its excellent electromagnetic absorption properties. ACS Appl. Mater. Interfaces **7**, 9776–9783 (2015)
20. J.S. Deng, S.M. Li, Y.Y. Zhou, L.Y. Liang, B. Zhao, Enhancing the microwave absorption properties of amorphous CoO nanosheet-coated Co (hexagonal and cubic phases) through interfacial polarization. J. Colloid Interface Sci. **509** 406–413. (2018)
21. G. Wu, Y. Cheng, Z. Yang, Z. Jia, H. Wu, L. Yang, H. Li, P. Guo, H. Lv, Design of carbon sphere/magnetic quantum dots with tunable phase compositions and boost dielectric loss behavior. Chem. Eng. J. **333**, 519–528 (2018)
22. H. Wu, G. Wu, Y. Ren, L. Yang, L. Wang, X. Li, Co^{2+}/Co^{3+} ratio dependence of electromagnetic wave absorption in hierarchical $NiCo_2O_4$-$CoNiO_2$ hybrids. J. Mater. Chem. C **3**, 7677–7690 (2015)
23. H. Wu, G. Wu, Y. Ren, X. Li, L. Wang, Multishelled metal oxide hollow spheres: easy synthesis and formation mechanism. Chem. Eur. J. **22**, 8864–8871 (2016)
24. G. Wu, H. Wu, K. Wang, C. Zheng, Y. Wang, A. Feng, Facile synthesis and application of multi-shelled SnO_2 hollow spheres in lithium ion battery. RSC Adv. **6**, 58069–58076 (2016)
25. L. Zhou, D. Zhao, X.W. Lou, Double-shelled $CoMn_2O_4$ hollow microcubes as high-capacity anodes for lithium-ion batteries. Adv. Mater. **24**, 745–748 (2012)
26. N. Venugopal, D.J. Lee, Y.J. Lee, Y.K. Sun, Self-assembled hollow mesoporous Co_3O_4 hybrid architectures: a facile synthesis and application in Li-ion batteries. J. Mater. Chem. A **1**, 13164–13170 (2013)
27. L. Shen, L. Yu, X.Y. Yu, X. Zhang, X.W. Lou, Self-templated formation of uniform $NiCo_2O_4$ hollow spheres with complex interior structures for lithium-ion batteries and supercapacitors. Angew. Chem. Int. Ed. **54**, 1868–1872 (2015)
28. A. Pan, H.B. Wu, L. Yu, X.W. Lou, Template-free synthesis of VO_2 hollow microspheres with various interiors and their conversion into V_2O_5 for lithium-ion batteries. Angew. Chem. Int. Ed. **52**, 2226–2230 (2013)
29. G. Zhang, X.W. Lou, General synthesis of multi-shelled mixed metal oxide hollow spheres with superior lithium storage properties. Angew. Chem. Int. Ed. **53**, 9041–9044 (2014)